

**Characterisation of the strain dependence of the Landau-Placzek ratio for  
distributed sensing**

*K. De Souza, P. C. Wait, and T. P. Newson*

*Optoelectronics Research Centre, University of Southampton, Highfield,  
Southampton, United Kingdom, SO17 IBJ.*

*E-mail: KDS@ORC.SOTON.AC.UK*

**Abstract**

This paper reports on the strain dependence of the Landau-Placzek ratio (LPR). This, together with the known temperature dependence of the LPR and the Brillouin frequency dependence on strain and temperature, may be used to form the basis of a combined distributed strain and temperature sensor.

*Introduction:* Previous work [1] has demonstrated the application of the LPR for temperature compensation in distributed strain sensing. This paper reports on the theoretical explanation and our measurement of the strain dependence of the LPR. With this knowledge of the LPR and the Brillouin frequency shift with temperature and strain [2], a combined distributed temperature and strain sensor is possible.

*Theory:* The dependence of Brillouin intensity with strain is given by [3]:

$$I_B = \frac{I_R T}{T_f (\rho v_a^2 B_T - 1)} \quad (1)$$

where  $I_R$  and  $I_B$  are the respective Rayleigh and Brillouin intensities,  $T_f$  is the fictive temperature,  $T$  is the ambient temperature and  $B_T$  is the isothermal compressibility. The acoustic velocity,  $v_a$ , is given by:

$$v_a = \sqrt{\frac{E(1-\sigma)}{\rho(1+\sigma)(1-2\sigma)}} \quad (2)$$

where,  $E$  is the Young's modulus,  $\sigma$  is the Poisson ratio and  $\rho$  is the density of silica. The Young's modulus of silica varies with strain according to the equation [4] :

$$E = E_o(1+5.75\epsilon) \quad (3)$$

where,  $E_o$  is the Young's modulus at zero strain and  $\epsilon$  is the tensile strain applied to the fibre. Substituting (2) and (3) into (4) and assuming that the Poisson ratio is independent of strain, yields:

$$I_B = \frac{k_1 I_R}{k_2(1+5.75\epsilon) - 1} \quad (4)$$

where  $k_1 = T/T_f$  and  $k_2 = E_o B_T(1-\sigma)/((1+\sigma)(1-2\sigma))$ .

*Experiment and results:* The experimental set up is shown in Fig. 1. The source [2] was a Q-switched erbium-doped fibre laser (QSL) with a centre wavelength of 1557 nm and pulse width of 100 ns. It was capable of providing both a narrow line width of 2 GHz needed for the separation of Rayleigh and Brillouin and a broadband of 2.5nm for the reduction of the coherent Rayleigh noise. The output from the QSL was monitored at photodetector PD1 via a 94/6 coupler. A 50/50 coupler, coupled 300 mW into the single mode sensing fibre. The latter

consisted of three sections with lengths of 350m, 110m, and 240m respectively. The first and last sections were unstrained. The middle section was wound on a pulley system to ensure strain uniformity. The Rayleigh and Brillouin signals were separated using an all-fibre Mach-Zehnder interferometer (free spectral range, FSR, of 22.3 GHz) and focussed on to photo detectors (PD2 and PD3) with a post-detection bandwidth of 1 MHz. Each detector was connected to a digital oscilloscope where signals were averaged 2048 times and stored.

The Stokes shift in the unstrained fibre was measured to be  $11.8 \pm 0.4$ GHz. The slight mismatch between the FSR of the MZ and the Stokes-Antistokes separation; together with the change in frequency shift with strain, were considered in determining the actual intensity change of the Brillouin signal with strain. Briefly, this entails locating the unstrained positions of the Brillouin components on the transfer function of the MZ and then tracking the path of the frequency shifts with strain. Using a Fabry-Perot interferometer, the frequency shift coefficient with strain was determined to be  $56 \pm 3$  KHz/ $\mu$ strain at an ambient temperature of  $293 \pm 0.5$  K.

Fig. 2 a, b, and c respectively show the superimposed and normalised backscattered broadband Rayleigh, Brillouin, and LPR traces under different strain conditions. Plots a, b, and c of Fig. 3 respectively show the experimentally obtained Brillouin intensities under different strains, contributions due to the FSR mismatch condition; and that due to strain only. Plot d shows the theoretical result using equation (4) and data from reference [3]. A strain coefficient, defined as the percentage change in the Brillouin intensity has been determined to be

$K_s = - (9.03 \pm 1.90) \times 10^{-4} \%$ / $\mu$ strain and hence the percentage LPR change per microstrain,  $LPR_s = (9.03 \pm 1.90) \times 10^{-4} \%$ / $\mu$ strain; the Rayleigh intensity being independent of strain. Fig. 4 shows the LPR versus  $\mu$ strain plot.

*Conclusion:* The LPR as a function of strain has been measured and found to be

$LPR_{\delta} = (9.03 \pm 1.90) \times 10^{-4} \% / \mu\text{strain}$  which agrees closely with the theoretical value of

$9.4 \times 10^{-4} \% / \mu\text{strain}$ . Hence all the Brillouin parameters necessary for the implementation of a combined distributed strain and temperature sensor are now known .

## References

- [1] WAIT, P.C., NEWSON, T.P.: 'Landau-Placzek ratio applied to distributed fibre sensing', *Optics Communications*, 1996, **122** (1) pp. 141-146.
- [2] DE SOUZA, K., LEES, G.P., WAIT, P.C., NEWSON, T.P.: 'A diode-pumped Landau-Placzek based distributed temperature sensor utilising an all-fibre Mach-Zehnder interferometer', *Electronics letters*, 1996, **32** (23) pp. 2174-2175.
- [3] SCHRODER, J., MOHR, R., MACEDO, P.B., MONTROSE, J.: 'Rayleigh and Brillouin scattering in  $K_2O-SiO_2$  glasses', *J. Am. Cer. Soc.*, 1973, **56** (10) pp.131.
- [4] BANSAL, P.B., DOREMUS, R. H.: 'Handbook of glass properties' (Academic Press, 1986)  
Ch. 2.

*Figure captions*

Figure 1: Experimental schematic of the distributed strain sensor.

Figure 2: Backscatter traces from the test fibre.

(a), (b) and (c) are the superimposed and normalised broadband backscattered Rayleigh signal, Brillouin, and LPR respectively.

Figure 3: (a) - intensity of Brillouin under different strain conditions.

(b) - contribution from mismatched FSR and Stokes-Antistokes separation.

(c) - intensity dependence on strain.

(d) - theoretical intensity dependence on strain

Figure 4: LPR vs microstrain.

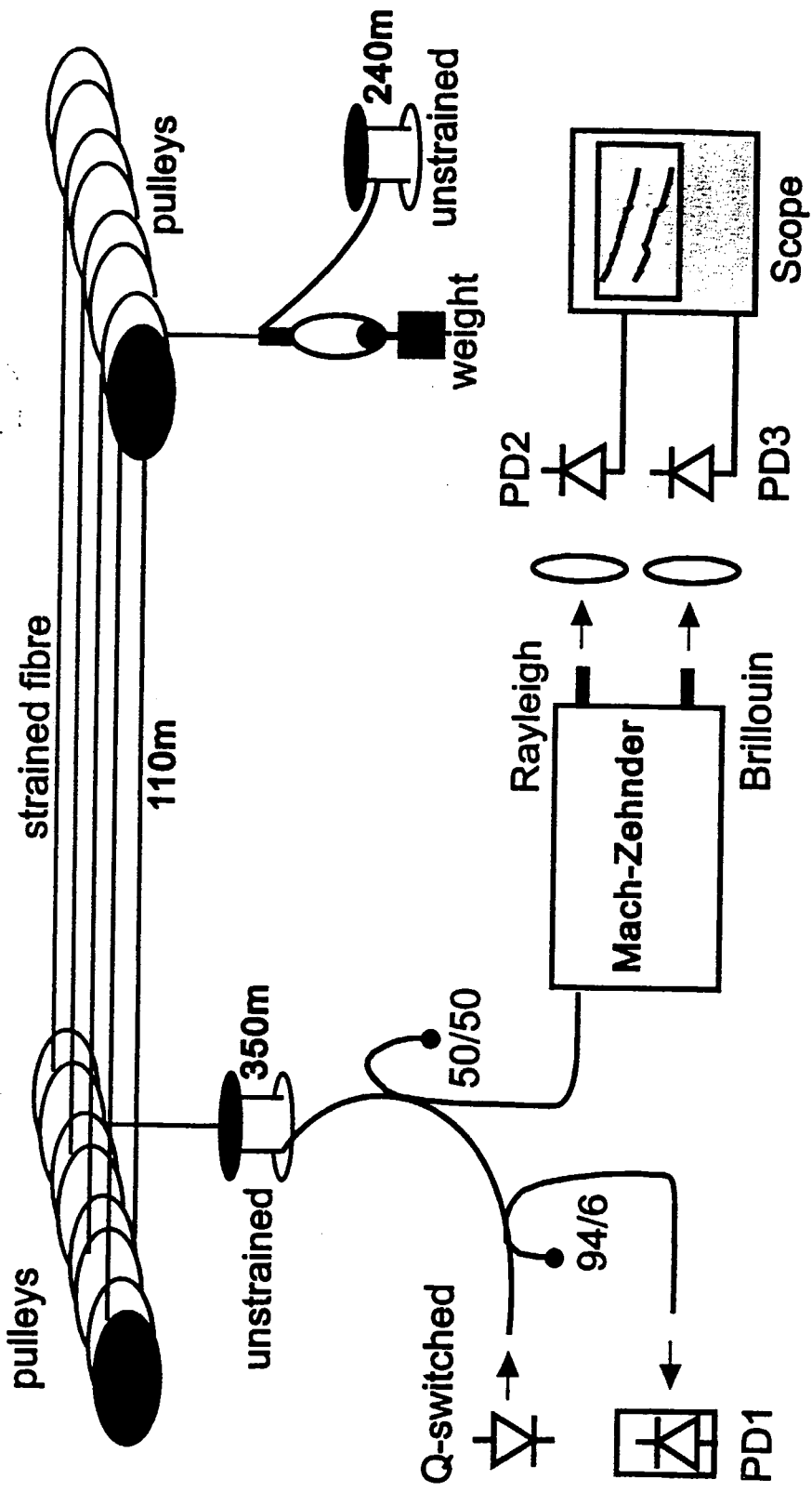


Figure 1

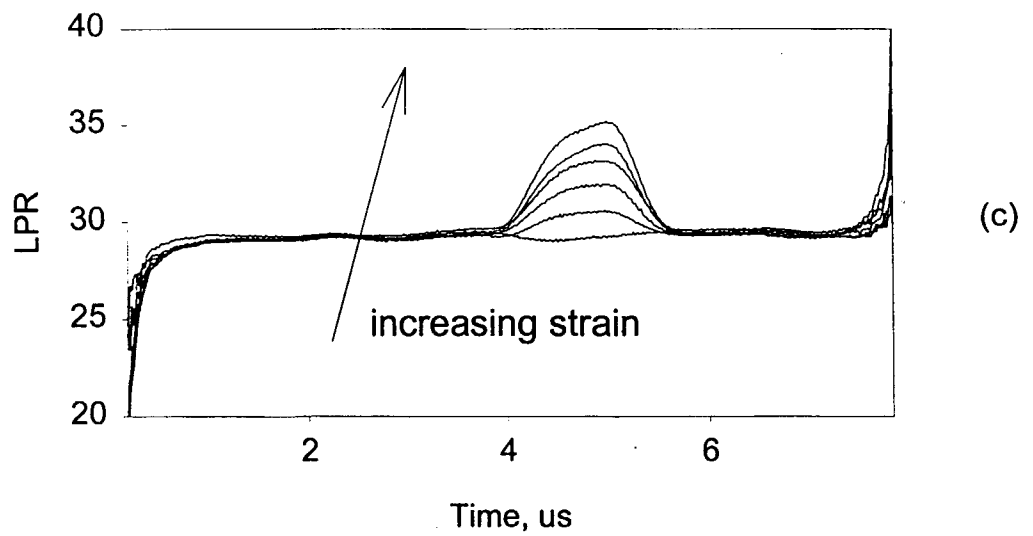
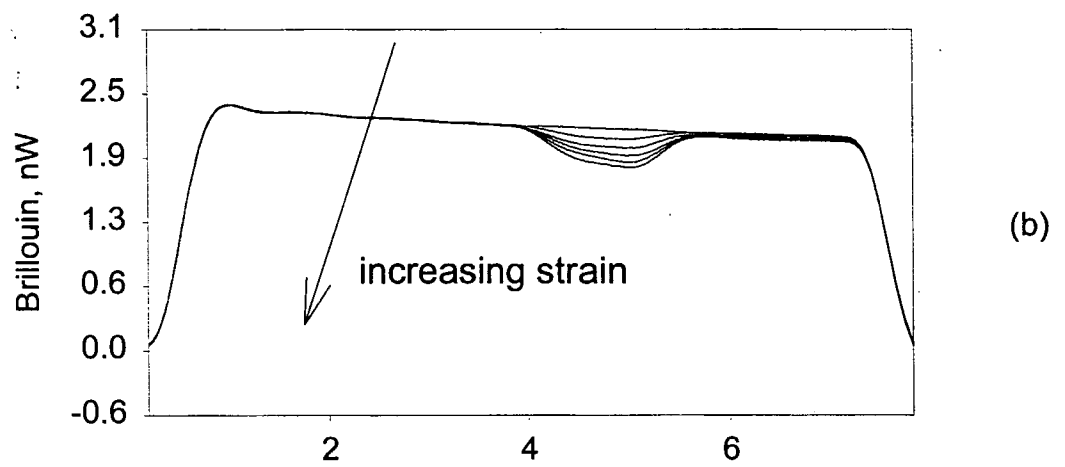
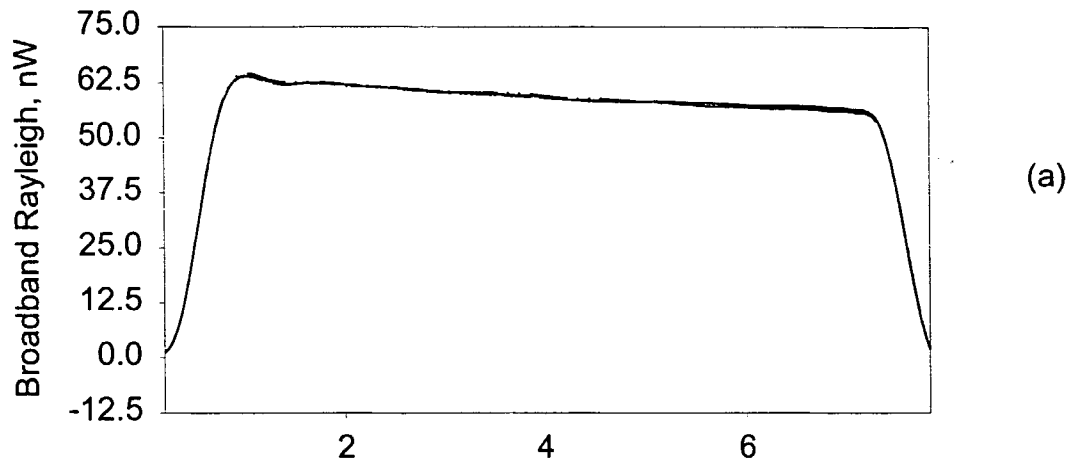


Fig. 2:(a) , (b), (c) Superimposed and normalized backscattered broadband Rayleigh signals, Brillouin signals, and LPR



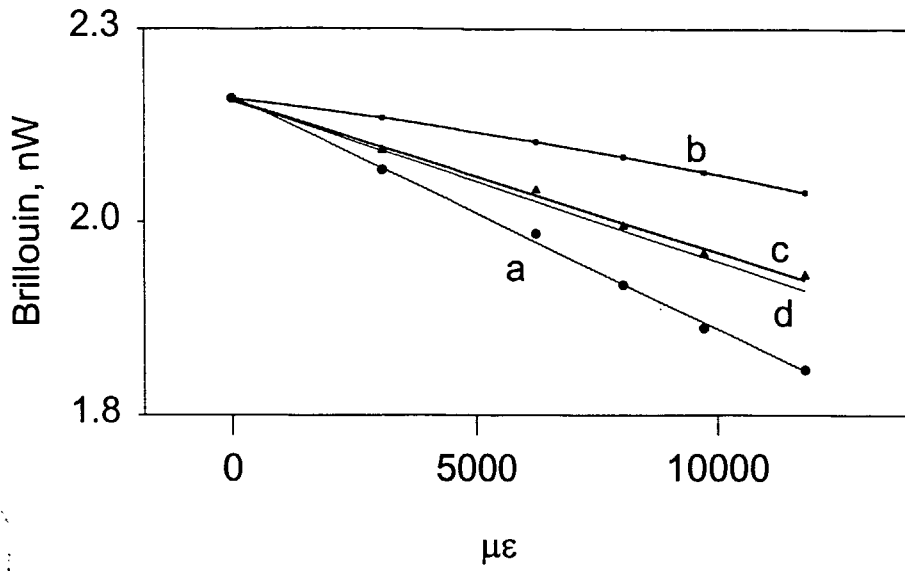


Fig. 3 (a): Experimentally obtained Brillouin intensities under different strains.  
 (b): Contribution due to FSR mismatch condition.  
 (c): Brillouin intensity dependence on strain only.  
 (d): Theoretical intensity dependence on strain.

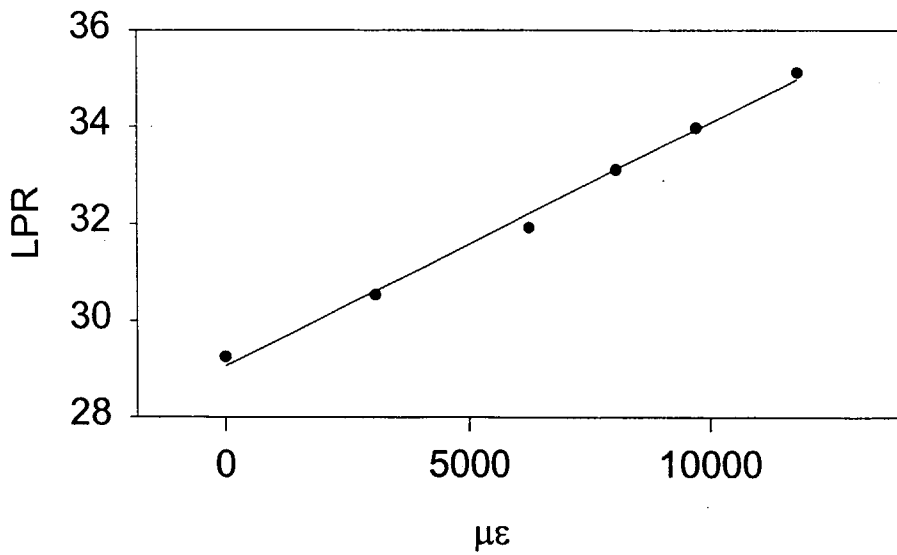


Fig. 4: Experimentally obtained LPR.